Imaging dynamics of exciton interactions and coupling in transition metal dichalcogenides

Torben L. Purz¹, Eric W. Martin², William G. Holtzmann³, Pasqual Rivera³, Adam Alfrey¹, Kelsey M. Bates¹, Hui Deng¹, Xiaodong Xu³, and Steven T. Cundiff¹

Department of Physics, University of Michigan, Ann Arbor, MI 48109-1040, USA
MONSTR Sense Technologies LLC, Ann Arbor, MI 48104, USA
Department of Physics, University of Washington, Seattle, Washington 98195-1560, USA

Abstract: We demonstrate coherent coupling between excitons in a MoSe₂/WSe₂ heterostructure, as well as rapid interlayer electron and hole transfer. We visualize the spatial homogeneity of the coupling in the presence of significant sample inhomogeneities. © 2022 The Author(s)

Transition metal dichalcogenides (TMDs) are regarded as a prime materials platform for applications ranging from solar-energy to quantum light-emitting diodes. In past years, the rapid charge transfer [1], coherent coupling [2], and interlayer excitons (ILEs) [3,4] have received considerable attention for their device applications potential. Depending on the proposed application and materials system, different physical parameters matter for the feasibility of the device. Among other things, dephasing times, charge transfer times and efficiency, ILE lifetimes, and coherent coupling strengths are quantities of interest. Here, we use multi-dimensional coherent spectroscopy (MDCS) [2] to show the existence of coherent coupling between excitons in MoSe₂ and WSe₂ monolayers stacked together to form a heterostructure, despite the presence of notable incoherent coupling in the form of charge transfer between the materials. Combining MDCS with imaging [5], we visualize complex local strain changes and map the robustness of charge transfer, coherent coupling, and ILE lifetimes across the heterostructure.

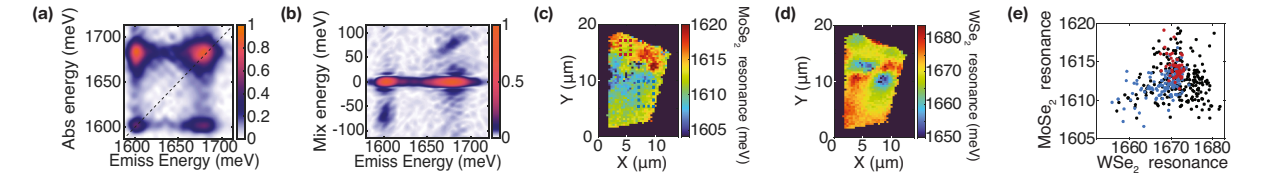


Fig. 1. (a) Low-power absorptive MDCS spectrum of a MoSe₂/WSe₂ heterostructure. (b) Zero-quantum spectrum showing signatures of coherent coupling between MoSe₂ and WSe₂ excitons. (c) MoSe₂ resonance energy map (d) WSe₂ resonance energy map (e) MoSe₂ vs. WSe₂ resonance energy, visualizing (anti-)correlation for the areas marked by (red)blue rectangles in (c).

A characteristic low-power MDCS spectrum for the sample is shown in Fig. 1(a). The two on-diagonal peaks (dashed line) correspond to the $MoSe_2$ and WSe_2 A-excitons. The coupling peaks can be caused by both coherent coupling and incoherent electron and hole (charge) transfer. We distinguish between coherent and incoherent coupling by performing zero-quantum spectroscopy [2], where instead of the absorption energy, the mixing energy between the two resonances is resolved. The zero-quantum spectrum shown in Fig. 1(b) clearly shows two peaks at mixing energies around ± 72 meV. This value equals the energy difference between $MoSe_2$ and WSe_2 resonances and is thus a clear indication of coherent coupling. This coupling between the excitons can be caused by static dipole-dipole, exchange interactions, or transition dipole (Förster) coupling [6], among other things. We have also previously resolved the incoherent charge transfer dynamics in this sample using MDCS [2].

Robustness of the coupling properties is paramount to device applications, but not self-evident given the complex strain environments common in TMD heterostructures. Demonstration of such an environment can be seen in Figs. 1(c-e). In Fig. 1(c) and (d) we map the resonance energy of the MoSe₂ and WSe₂ exciton respectively. Broad resonance shifts can be observed for both intralayer excitons. Noticeably, the resonance shifts are globally uncorrelated - with a Pearson correlation coefficient of $\rho = 0.10$ for all data points in Fig. 1(e), but locally strongly (anti)-correlated. This is evident from the resonance energies for the red (blue) rectangle in Fig. 1(c), which are plotted in red (blue) in Fig. 1(e). For the blue rectangle, a strong correlation (ρ =0.54) can be observed. For the red rectangle, a strong anti-correlation (ρ =-0.43) can be observed. Since encapsulation, heterostructure formation, and strain commonly shift the resonances in both monolayers in the same direction, these observations point to

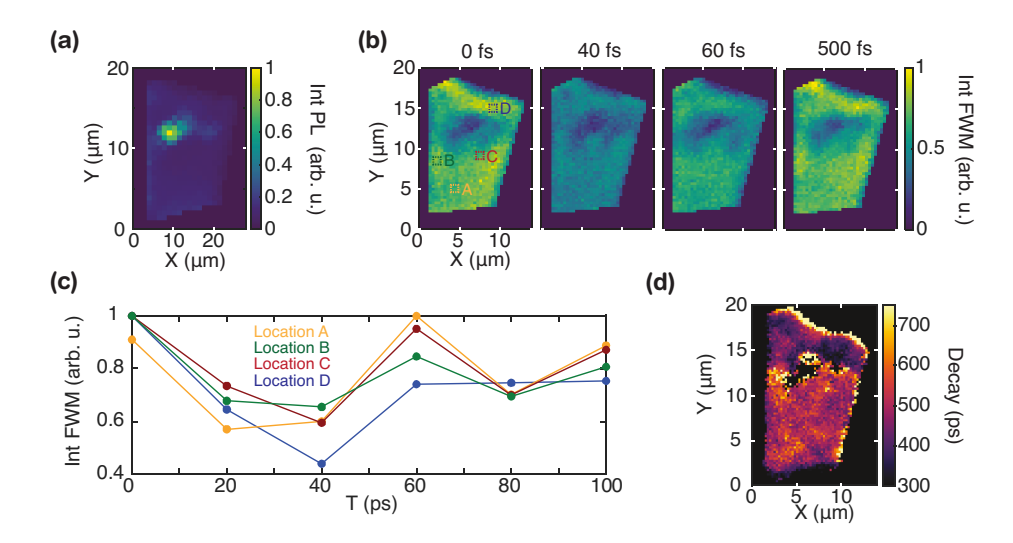


Fig. 2. (a) Integrated PL map of the ILE. (b) Integrated FWM signal map for the $MoSe_2/WSe_2$ coupling peak for varying T delay. (c) T-dependent integrated FWM signal for the $MoSe_2/WSe_2$ coupling peak for four sample points marked in (b) indicated by the corresponding color. (d) Fourwave mixing decay map, an indirect measure of interlayer exciton lifetime.

complex local strain dynamics with the two materials experiencing different strain. The assignment to strain is further supported by the spatially inhomogeneous interlayer exciton photoluminescence (PL) shown in Fig. 2(a).

Despite these strain-induced changes to the sample response, imaging MDCS experiments show a mostly homogeneous four-wave mixing (FWM) strength across the sample, apart from the high strain area of maximum PL emission. In Fig. 2(b) we plot the integrated FWM amplitude of the MoSe₂/WSe₂ coupling peak (lower right in Fig. 1(a)) as a function of pump-probe delay T. Apart from the mostly homogeneous FWM strength, the T-dependence allows us to visualize the robustness of coherent coupling and charge transfer. The initial decay between T=0 fs and 40 fs and partial recovery for 60 fs is a signature of the coherent coupling oscillations. The rise between 100 fs and 500 fs can be assigned to hole transfer from the MoSe₂ to the WSe₂. Given that the absolute strength of the signal changes, but not the spatial profile, these measurements establish robustness of coherent coupling and charge transfer towards the local strain dynamics. This is corroborated by the full T-dependent data plotted for select sample points in Fig. 2(c), where only the upper area of the sample shows slightly weaker coupling. This is in line with the FWM decay map plotted in Fig. 2(d), an indirect measure of the ILE lifetime. The map shows on average lower decay times at the top of the sample which we associate with increased layer spacing. Nonetheless, the robustness of the sample properties is surprising given the sensitivity of the couplings and ILEs to numerous sample parameters, including twist angle and layer separation, the latter one of which should be affected by the complex strain dynamics.

The future of TMDs in device applications is inherently coupled to the scalability and quality of fabricated devices. This work shows reproducibility of crucial physical properties across the sample, laying the groundwork and strengthening the case for TMDs as a next-generation materials platform.

References

- 1. V. R. Policht, M. Russo, F. Liu, C. Trovatello, M. Maiuri, Y. Bai, X. Zhu, S. Dal Conte, and G. Cerullo, "Dissecting Interlayer Hole and Electron Transfer in Transition Metal Dichalcogenide Heterostructures via Two-Dimensional Electronic Spectroscopy," Nano Lett. 21, 4738–4743 (2021).
- 2. T. L. Purz, E. W. Martin, P. Rivera, W. G. Holtzmann, X. Xu, and S. T. Cundiff, "Coherent exciton-exciton interactions and exciton dynamics in a MoSe₂/WSe₂ heterostructure," Phys. Rev. B **104**, L241302 (2021).
- 3. P. Rivera, J. Schaibley, A. Jones, J. Ross, S. Wu, G. Aivazian, P. Klement, K. Seyler, G. Clark, N. Ghimire, J. Yan, D. Mandrus, W. Yao, and X. Xu, "Observation of long-lived interlayer excitons in monolayer MoSe₂-WSe₂ heterostructures," Nat Commun **6**, 6242 (2015).
- 4. A. Ciarrocchi, D. Unuchek, A. Avsar, K. Watanabe, T. Taniguchi, and A. Kis, "Polarization switching and electrical control of interlayer excitons in two-dimensional van der waals heterostructures," Nat. Photonics 13, 131–136 (2019).
- 5. T. L. Purz, S. T. Cundiff, and E. W. Martin, "Lock-in detector for accelerated nonlinear imaging," Opt. Lett. 46, 4813–4816 (2021).
- 6. B. Kasprzak, J.and Patton, V. Savona, and W. Langbein, "Coherent coupling between distant excitons revealed by two-dimensional nonlinear hyperspectral imaging," Nat. Photonics p. 57–63 (2011).